Supporting Information

Dual Mechanism with Graded Energy Storage in Long-term Aqueous Zinc-Ion Batteries Achieved by Polymer/Vanadium Dioxide Cathode

Zhihang Song,[#a] Yi Zhao,[#b] Huirong Wang,[a] Anbin Zhou,[a] Xiaoyu Jin,[a] Yongxin Huang,*[ac] Li Li,[acd] Feng Wu,[acd] Renjie Chen*[acd]

a Beijing Key Laboratory of Environmental Science and Engineering, School of Materials Science & Engineering, Beijing Institute of Technology, Beijing 100081, China, E-mail: chenrj@bit.edu.cn (R. Chen); huangyx@bit.edu.cn (Y. Huang).

b State Key Laboratory of Chemical Engineering, College of Chemistry, Beijing University of Chemical Technology, Beijing 100029, China.

c Advanced Technology Research Institute (Jinan), Beijing Institute of Technology, Jinan 250300, China.

d Collaborative Innovation Center of Electric Vehicles in Beijing, Beijing 100081, China

 # These authors contributed equally to this work

Experimental Section/Methods

Experimental Procedures

In a typical synthesis, 0.364 g of V_2O_5 powder was dissolved in 60 mL deionized water, continue stirring until V_2O_5 is completely dissolved and the solution is aurantium. A total of 0.2088 g NDA powder was added in two separate batches, stirring continuously for 40 minutes, and the solution turned chartreuse. Transfer the solution to 100ml Teflon lining and hydrothermal, the temperature was raised to 140 °C for 24 h. After the hydrothermal treatment, the autoclave was cooled down to room temperature naturally and the precipitate was collected by vacuum filtration, washed with deionized water, and dried at 80 °C.

Material characterization

The morphology of the electrode was conducted on Hitachi S4800 field emission scanning electron microscope with an acceleration voltage of 5 kV. The TEM data of the samples were collected by Thermo Fisher Talos F200S G2. The crystalline structure of the active materials was characterized by X-ray diffraction (XRD) on Rigaku SmartLab SE with a Cu Kα source. Raman spectroscopy was acquired on ThermoFisher DXR2 xi with a 532 nm laser source. Infrared spectra were obtained on Thermo Scientific Nicolet iS50 FTIR. The chemical compositions of the active materials were measured by X-ray photoelectron spectroscopy (XPS) on Thermo Scientific ESCALAB 250Xi. The content of elements in the powder was measured by ICP-OES/MS on Agilent 5110(OES).

Electrode fabrication and electrochemical testing

The as-prepared VO@NDA powder were directly mixed with conductive carbon black conductive agent and PVDF binder at a ratio of 7:2:1, and a small amount of 1-Methyl-2-pyrrolidinone (NMP) was added as solvent. The slurry is coated on the carbon cloth collector fluid and dried as cathodes for aqueous ZIBs. The VO_2 and V_2O_5 cathodes are prepared in a similar manner. The anode is a zinc foil with a diameter of 11 mm and a thickness of 70 μm. Two electrolytes, 2M $Zn(CF_3SO_3)_2$ aqueous solution with and without 0.2M KI, were prepared for comparison, named otf@I and otf. The separator is a glass fiber membrane with a diameter of 19 mm. The above materials were assembled into CR2032-type coin cell in order to be tested. CV measurements were conducted using a CorrTest CS2350H electrochemical workstation (Wuhan CorrTest Instrument Corp., Ltd. China) at various scan rates (0.6, 0.8, 1.0, 1.2, 1.4 and 1.6 mV s^{-1}) with a scan range of 0.4–1.6 V. EIS was measured by a CHI660E

electrochemical workstation at a frequency of 100 kHz–0.01 Hz.

Analytical method

The GITT and galvanostatic charge/discharge measurements were executed on Neware battery testing system with a voltage range of 0.4 to 1.6 V. For the GITT experiment, a constant current density (0.5 A g^{-1}) was applied to the cell for 30 seconds, followed by 5 minutes of open-circuit relaxation, and the steps were repeated until the voltage reached 0.4 V or 1.6 V. The diffusion coefficient of Zn^{2+} was calculated according to the following equation:

$$D = \frac{4}{\pi\tau}\left(\frac{R_s}{3}\right)^2\left(\frac{\Delta E_s}{\Delta E_t}\right)^2$$

where τ refers to the duration time (30 s in this test) of the current pulse, R_s is the radius of the active material powder, ΔE_s and ΔE_t correspond to the steady-state potential change (V) caused by the current pulse and the direct voltage change (V) before relaxation, respectively, as shown in Fig. S15.

DFT method

All the DFT calculations were conducted based on the Vienna Ab-inito Simulation Package (VASP). The exchange-correlation effects were described by the Perdew-Burke-Ernzerhof (PBE) functional within the generalized gradient approximation (GGA) method. The core-valence interactions were accounted by the projected augmented wave (PAW) method. The energy cutoff for plane wave expansions was set to 480 eV, and the 3×3×1 Monkhorst-Pack grid k-points were selected to sample the Brillouin zone integration. The vacuum space is adopted 15 Å above the surfaces to avoid periodic interactions. The structural optimization was completed for energy and force convergence set at 1.0×10^{-4} eV and 0.02 eV $Å^{-1}$, respectively.

The adsorption energy can be calculated according to the following formula:

$$Eads=E(A+B)-E(A)-E(B)$$

where Eads represents the adsorption energy, E(A+B) is the calculated energy of adsorption configuration, E(A) and E(B) mean the calculated energy of substrate and adsorbent respectively.

The Gibbs free energy change (ΔG) of each step is calculated using the following formula:

$$\Delta G=\Delta E+\Delta ZPE-T\Delta S$$

where ΔE is the electronic energy difference directly obtained from DFT calculations, ΔZPE is the zero point energy difference, T is the room temperature (298.15 K) and ΔS is the entropy change. ZPE could be obtained after frequency calculation by:

$$ZPE = \frac{1}{2}\sum h\nu_i$$

And the TS values of adsorbed species are calculated according to the vibrational frequencies:

$$TS = k_BT\left[\sum_k \ln\left(\frac{1}{1 - e^{-h\nu/k_BT}}\right) + \sum_k \frac{h\nu}{k_BT}\frac{1}{(e^{h\nu/k_BT} - 1)} + 1\right]$$

Supplementary Figures and Tables

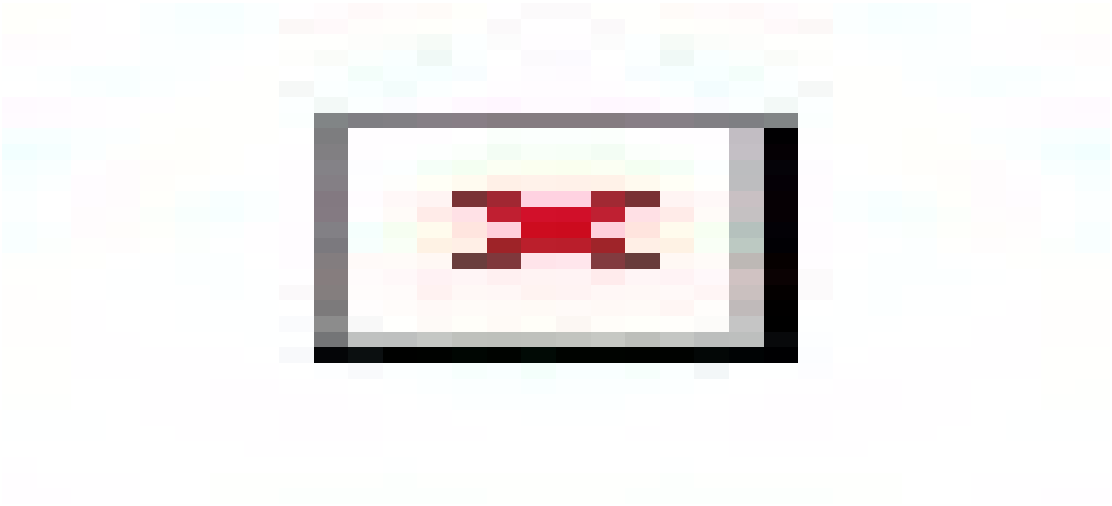

Fig. S1 Morphology and composition of VO@NDA, mapping of V, O, C, and N elements.

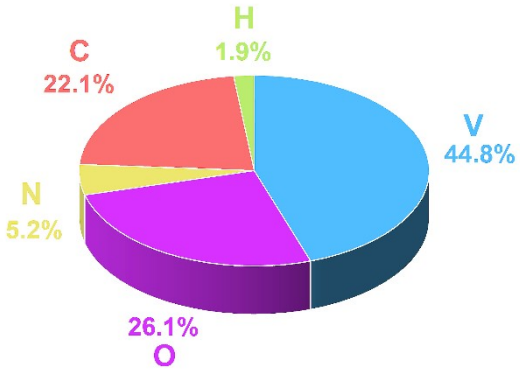

Fig. S2 The element proportion of VO@NDA.

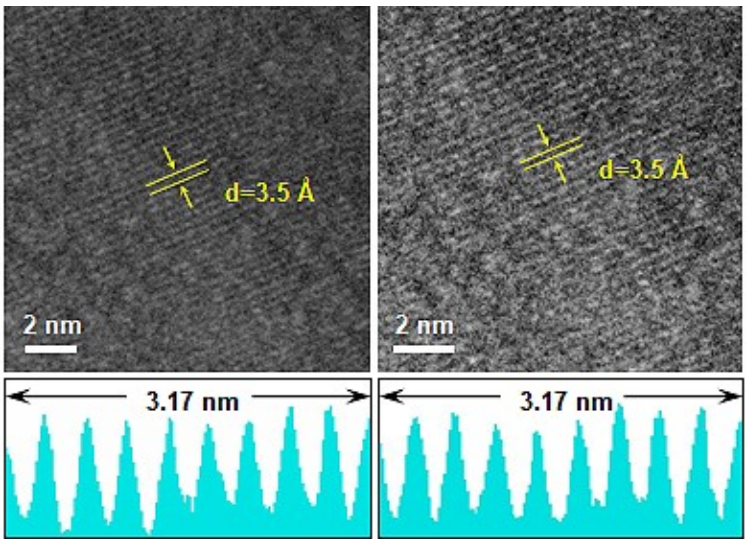

Fig. S3 HRTEM image of VO@NDA.

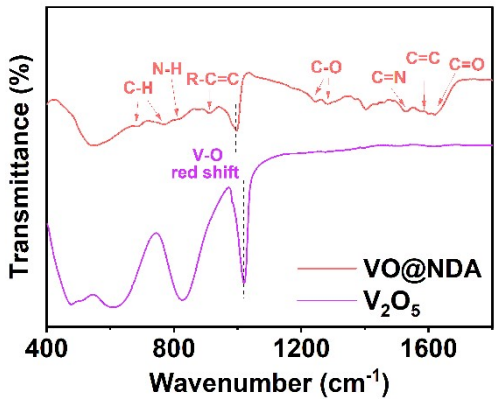

Fig. S4 FTIR spectra of V_2O_5 and VO@NDA

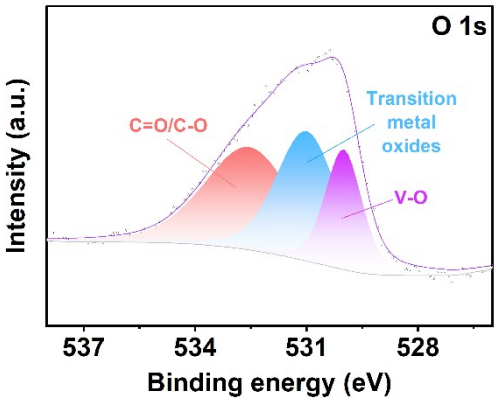

Fig. S5 O 1s high-resolution XPS spectra for the VO@NDA.

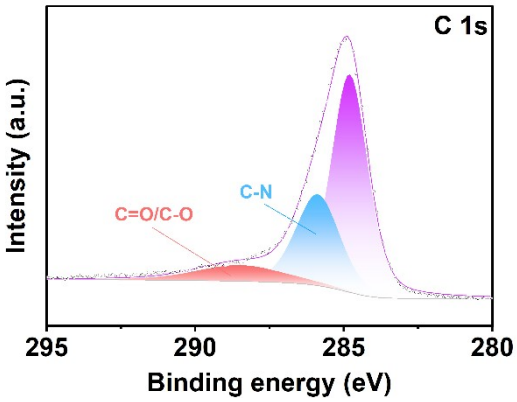

Fig. S6 C 1s high-resolution XPS spectra for the VO@NDA.

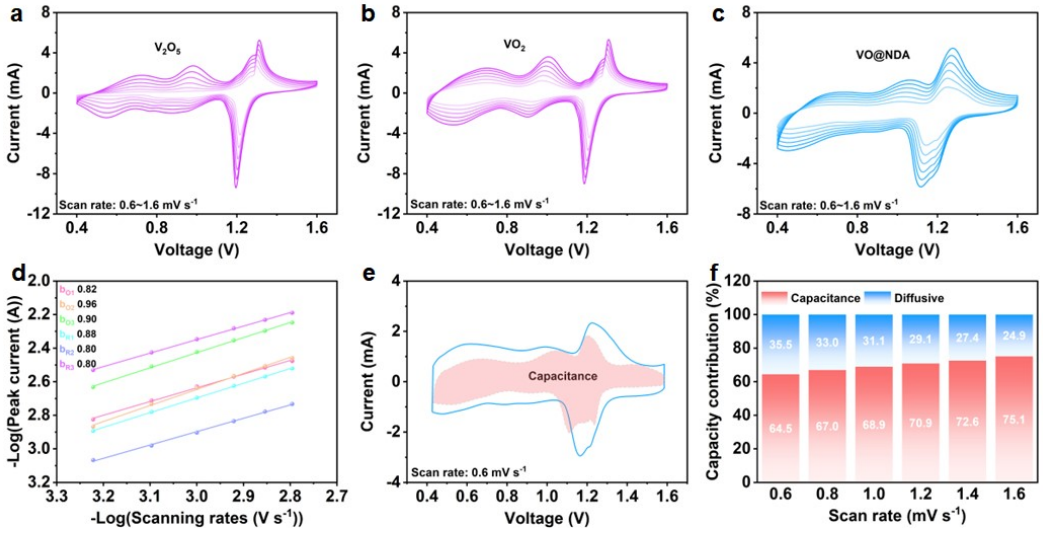

Fig. S7 The unprocessed CV curves of (a) V_2O_5, b) VO_2 and (c) VO@NDA at different scan rates. (d) log (i) versus log (v) plots at specific peak currents of VO@NDA. (e) Contribution area distribution of pseudo-capacitance of VO@NDA. (f) The contribution ratio of the pseudo-capacitance and diffusion-limited capacities at different scan rates of VO@NDA.

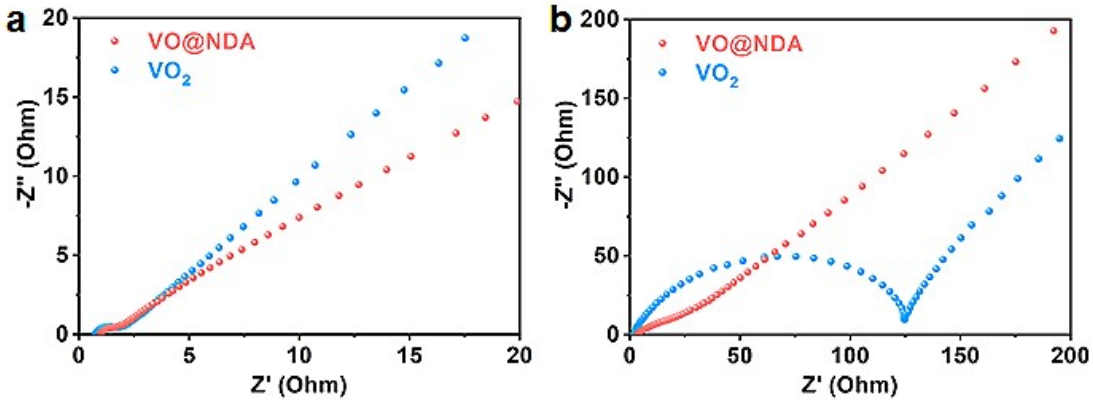

Fig. S8 (a) EIS profiles of the VO2 and VO@NDA cathodes in $Zn(CF_3SO_3)_2$ electrolytes without 0.2M KI, respectively; (b) EIS profiles of the VO_2 and VO@NDA cathodes in $Zn(CF_3SO_3)_2$ electrolytes with 0.2M KI, respectively.

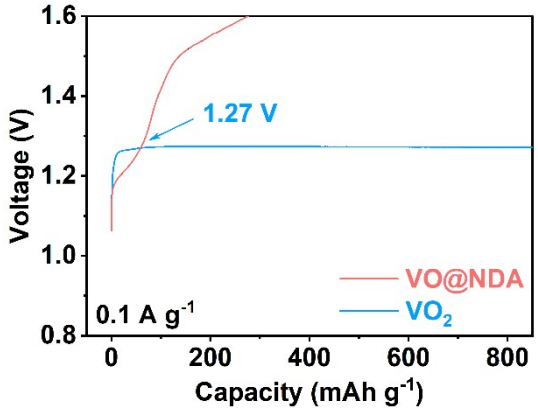

Fig. S9 Charge and discharge curve of VO@NDA and VO_2 at 0.1A g^{-1}, respectively.

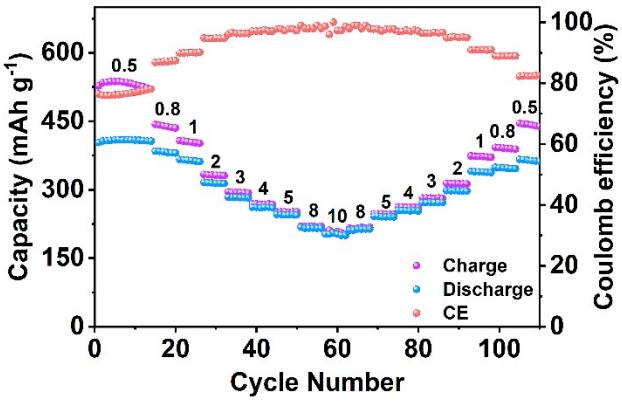

Fig. S10 Rate performance test of VO_2.

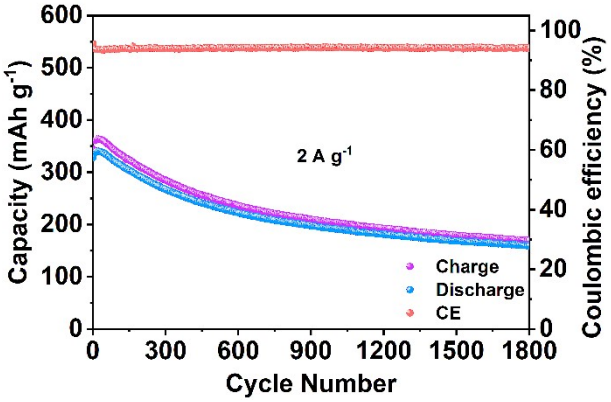

Fig. S11 Cycling stability test curve of VO_2 at 2 A g^{-1}.

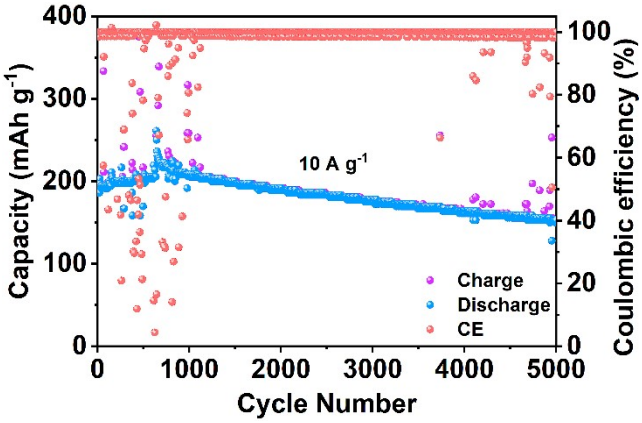

Fig. S12 Cycling stability test curve of VO_2 at 10 A g^{-1}.

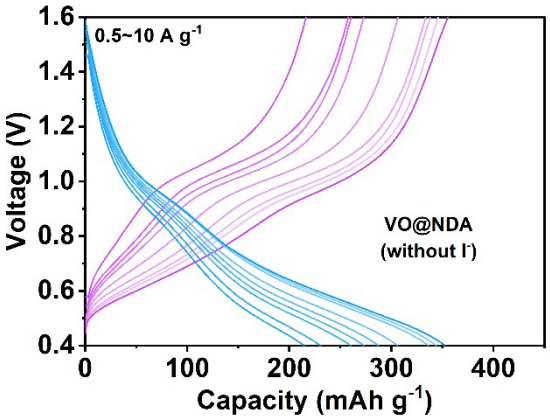

Figure S13. Charge and discharge curve of VO@NDA at 0.5~10 A g^{-1} without I^- contained electrolytes.

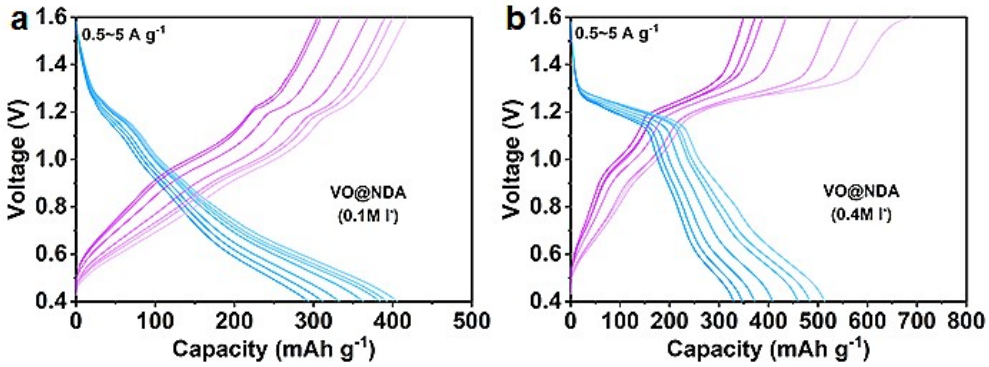

Figure S14. The charge and discharge curves of VO@NDA cathodes at (a) 0.1M and (b) 0.4M KI, respectively.

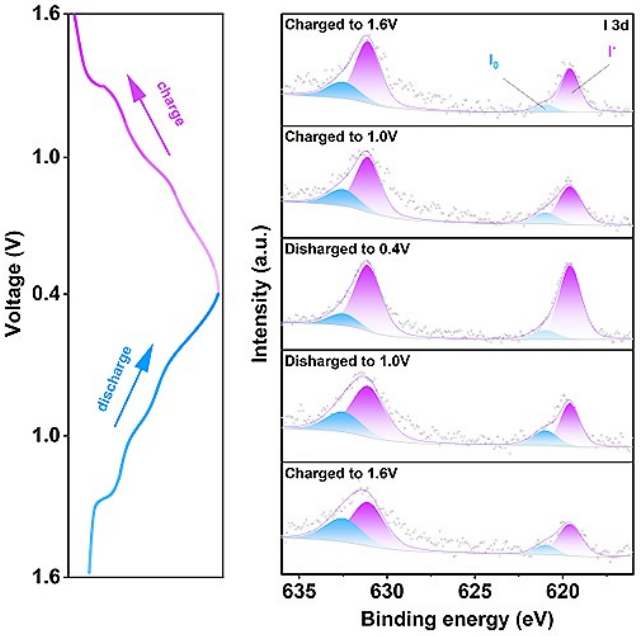

Fig. S15 I 3d high-resolution XPS spectra for the VO_2 electrodes.

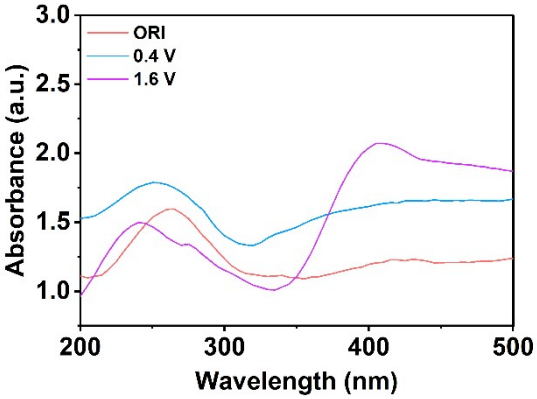

Fig. S16 UV spectra of VO@NDA electrodes.

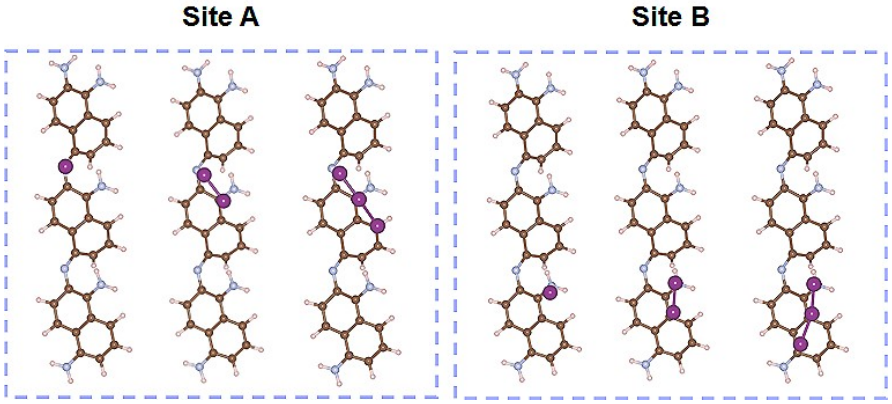

Fig. S17 Illustration of adsorption of I^-,I_3^-,I_2 at site A and B.

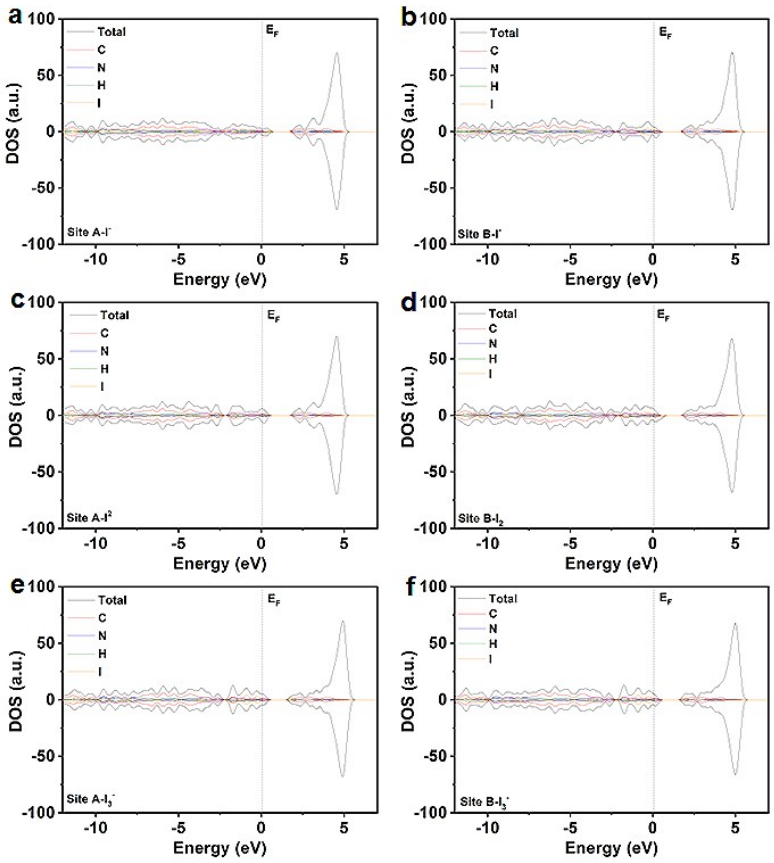

Fig. S18 DOS diagram of SiteA and B adsorbing I^-,I_3^-,I_2 states

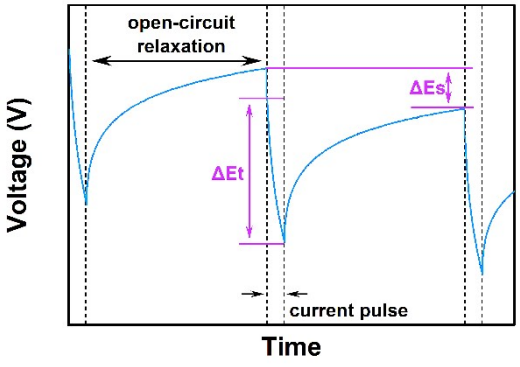

Fig. S19 Schematic illustration of selected steps of the GITT curve during discharging.

Table S1 Median voltage comparison of modified vanadium oxides.

Cathode	Capacity (V)	Reference
VO_2	0.55	1
$Mg_{0.34}V_2O_5\ nH_2O$	0.6	2
$Ni_{0.25}V_2O_5\ nH_2O$	0.603	3
$V_5O_{12}\ 6H_2O$	0.61	4
PANI-V_2O_5	0.65	5
$VO_2\ 0.45H_2O$	0.655	6
V_2O_5@PEDOT	0.66	7
PEDOT-$NH_4V_3O_8$	0.68	8
w-VO_2	0.692	9
PANI-V_2O_5	0.7	10
H-doped of VO_2	0.7	11
$Mn_{0.15}V_2O_5\ nH_2O$	0.72	12
$NaV_3O_8\ 1.5H_2O$	0.74	13
$ZnV_6O_{16}\cdot 8H_2O$	0.745	14
This work	0.76	

References

1 Z. Li, S. Ganapathy, Y. Xu, Z. Zhou, M. Sarilar, M. Wagemaker, *Advanced Energy Materials* **2019**, 9, 1900237.

2 F. Ming, H. Liang, Y. Lei, S. Kandambeth, M. Eddaoudi, H. N. Alshareef, *ACS Energy Letters* **2018**, 3, 2602.

3 J. Li, K. McColl, X. Lu, S. Sathasivam, H. Dong, L. Kang, Z. Li, S. Zhao, A. G. Kafizas, R. Wang, D. J. L. Brett, P. R. Shearing, F. Corà, G. He, C. J. Carmalt, I. P. Parkin, *Advanced Energy Materials* **2020**, 10, 2000058.

4 N. Zhang, M. Jia, Y. Dong, Y. Wang, J. Xu, Y. Liu, L. Jiao, F. Cheng, *Advanced Functional Materials* **2019**, 29, 1807331.

5 S. Liu, H. Zhu, B. Zhang, G. Li, H. Zhu, Y. Ren, H. Geng, Y. Yang, Q. Liu, C. C. Li, *Advanced Materials* **2020**, 32, 2001113.

6 K. Zhu, T. Wu, S. Sun, W. van den Bergh, M. Stefik, K. Huang, *Energy Storage Materials* **2020**, 29, 60.

7 Z. Yao, Q. Wu, K. Chen, J. Liu, C. Li, *Energy & Environmental Science* **2020**, 13, 3149.

8 D. Bin, W. Huo, Y. Yuan, J. Huang, Y. Liu, Y. Zhang, F. Dong, Y. Wang, Y. Xia, *Chem* **2020**, 6, 968.

9 J. Yang, H. Tian, Y. Li, H. Li, S. Li, H. Yang, M. Ding, X. Wang, P.-Y. Chen, *Energy Storage Materials* **2022**, 53, 352.

10 S. Chen, K. Li, K. S. Hui, J. Zhang, *Advanced Functional Materials* **2020**, 30, 2003890.

11 K. Guan, K. Duan, G. Yang, L. Tao, H. Zhang, H. Wan, R. Yang, J. Zhang, H. Wang, H. Wang, *Materials Today Advances* **2022**, 14, 100230.

12 H. Geng, M. Cheng, B. Wang, Y. Yang, Y. Zhang, C. C. Li, *Advanced Functional Materials* **2020**, 30, 1907684.

13 F. Wan, L. Zhang, X. Dai, X. Wang, Z. Niu, J. Chen, *Nature Communications* **2018**, 9, 1656.

14 K. Zhu, W. Jiang, Z. Wang, W. Li, W. Xie, H. Yang, W. Yang, *Angewandte Chemie International Edition* **2023**, 62, e202213368.